

# Characterization of Miller-Similar Silica Sands for Laboratory Hydrologic Studies

M. H. Schroth,\* S. J. Ahearn, J. S. Selker, and J. D. Istok

## ABSTRACT

The use of well-characterized porous media can simplify and improve the efficiency of laboratory subsurface flow and transport experiments. The objective of this study was to present a comprehensive set of hydrologically relevant properties for a unique set of commercially available silica sands. Features of sands selected for characterization included high sphericity, high batch-to-batch consistency, Miller-similarity, and availability in large quantities. Samples of four different sand grades (12/20, 20/30, 30/40, and 40/50 sieve sizes) were characterized for physical properties, chemical composition, water retention, three-phase air–non-aqueous-phase liquid (NAPL)–water saturation–pressure relationships for water and a model NAPL, Soltrol 220, and saturated and unsaturated hydraulic conductivity. Properties common to all sand grades included high chemical purity and low organic matter content. Water retention curves featured well-defined air entry pressures and the Miller-similarity of the media was demonstrated for both static and dynamic properties. During water retention measurements, we determined that the common assumption of a uniform vertical water content distribution in retention cells can result in significant errors in uniform porous media. A numerical correction procedure was developed and successfully applied to correct fitted water retention curve parameters, illustrating that potential errors of up to 70% in volumetric water content are made without proper analysis. The characterization data for the four sand grades presented here should facilitate their use in a wide range of laboratory flow and transport studies.

**F**LUID FLOW and solute transport are critical processes related to contamination, remediation, and conservation of soil and groundwater resources. Countless experiments are being conducted to study the movement of single fluid phases, i.e., water, NAPLs, and gases, multiple fluid phases, and contaminants in subsurface environments. Fluid flow and solute transport problems frequently involve complex physical, chemical, and biological processes. Laboratory experiments in physical models, chambers, and columns are often conducted to limit scientific studies to the investigation of specific phenomena.

The selection of porous media is an important initial step for conducting laboratory subsurface hydrologic experiments. Availability, sometimes in large quantities, low cost, and well-defined physical, chemical, and biological properties are desired features of porous media. In addition, the porous medium should be representative of the natural environment.

To interpret experimental results, knowledge of basic hydrologic properties is required. Obtaining these properties often requires specialized equipment and techniques that can be time consuming and expensive. For many applications, the use of previously characterized media may be desirable. However, for previously charac-

terized media to be reliable, it must possess high batch-to-batch consistency and uniformity in the desired properties. Therefore, commercial processing is usually required to produce this level of consistency and uniformity.

The primary objective of this study was to present a comprehensive set of hydrologically relevant properties for commercially available silica sands so that the media could be employed by the broad scientific community. In addition, we wanted to verify that the four grades of sand characterized were hydrodynamically similar in the sense of Miller and Miller (1956). Finally, we wanted to develop a more accurate approach to interpreting water retention data obtained in retention cells for coarse, uniform-textured porous media.

## MATERIALS AND METHODS

### Porous Media and Liquids

The porous media selected for characterization were four grades of silica sand (12/20, 20/30, 30/40, and 40/50 sieve sizes), available in large quantities from Unimin Corporation<sup>1</sup> (Le Sueur, MN), under the trade name Accusand. Accusand grades were obtained prewashed (with water) and presieved by the manufacturer. Prior to conducting characterization experiments, all Accusand grades were rinsed with distilled water to remove fine dusts. The Accusand grades were then oven dried at 50°C. No further treatment was employed.

Liquids used for the characterization of Accusand grades were distilled water and Soltrol 220, hereafter referred to as Soltrol, a light NAPL manufactured by Phillips Petroleum Company (Bartlesville, OK). Soltrol is a mixture of branched C<sub>13</sub> to C<sub>17</sub> alkanes with a specific gravity of 0.81. Its components can be found in a variety of petrochemical products, e.g., diesel fuel. Negligible water solubility, very low volatility at room temperature, as well as a low health hazard are reasons for the extensive use of Soltrol as a model NAPL in multiphase flow studies (e.g., Cary et al., 1994; Lenhard, 1992).

### Physical and Chemical Characterization

Sieve analyses and determination of sphericity for four Accusand grades were performed by the manufacturer using standard methods (ASTM, 1987; American Petroleum Institute, 1986). Particle densities were measured in our laboratory by He pycnometry (Ayrat et al., 1992) using an ACCUPYC Model 1330 pycnometer (Micromeritics Instrument Corp., Norcross, GA).

The cation-exchange capacities for the four Accusand grades were determined by extraction (Page et al., 1982) and ICP/AAS (U.S. Environmental Protection Agency, 1986). Total Fe, total Cd, total Cu, total Pb, total Mn, and total Zn contents were determined by HNO<sub>3</sub> digestion and ICP/AAS (U.S. Environmental Protection Agency, 1986). Iron oxide (Fe<sub>2</sub>O<sub>3</sub>) content was determined by extraction (Page et al., 1982) and ICP/

M.H. Schroth and J.D. Istok, Dep. of Civil Engineering, and S.J. Ahearn and J.S. Selker, Dep. of Bioresource Engineering, Oregon State Univ., Corvallis, OR 97331. Received 11 Sept. 1995. \*Corresponding author (schrothm@ucs.orst.edu).

<sup>1</sup> Reference to trade names or companies is made for information purposes only and does not imply endorsement by Oregon State University or the US-DOE.

**Abbreviations:** NAPL, non-aqueous-phase liquid; ICP/AAS, inductively coupled plasma atomic absorption spectrophotometry; S-P, saturation-pressure.

AAS (U.S.Environmental Protection Agency, 1986). Organic C content was determined from sand samples pretreated with H<sub>3</sub>PO<sub>4</sub> using a N-C-S analyzer (Artiola, 1990).

**Water Retention Measurements**

Water retention data were obtained using a three-phase retention cell as described by Lenhard and Parker (1988). The retention cell consisted of four acrylic rings joined together with silicone sealant (Fig. 1a). Four ceramic rings were glued to the inside of the retention cell's acrylic rings. Two of the ceramic rings (the "NAPL rings") were chemically treated with chlorotrimethylsilane to render them hydrophobic to conduct only NAPL (Lenhard, 1992). The other two rings (the "water rings") were not treated and were used to conduct water. Fittings connected to cavities behind the ceramic rings allowed free liquid movement into and out of the retention cell. Plastic tubing was used to connect the water and NAPL rings to pressure transducers, burettes, and vacuum-pressure regulators. In this manner, water and NAPL volumes and pressures could be measured independently. The pressure transducers were kept in a fixed position relative to the retention cell throughout the measurements.

Prior to conducting water retention measurements, the water pressure transducer was calibrated with the free water surface elevation set to the upper sand surface (Fig. 1a). All subsequent pressure measurements were thus made in reference to this location. To conduct water retention measurements, the porous

medium was packed by pouring sand into the retention cell under water while continuously stirring to establish an initial condition of complete (100%) water saturation. Water was subsequently drained from the porous media by applying an external vacuum to the water rings; the volume of water drained was determined using a burette. Measurements of capillary pressure head as a function of the cumulative volume of water drained were recorded when all flow from the cell had ceased. During water retention measurements, the tubing to the NAPL rings was clamped off.

For each cumulative increment of water drained from the porous media  $V_{w,i}$ , the corresponding volumetric water contents  $\theta_i$  of the porous media were computed using:

$$\theta_i = (V_i\phi - V_{w,i})/V_i \quad [1]$$

where  $V_i$  is the total volume of the retention cell (Fig. 1a),  $\phi$  is the porosity of the packed sand, and subscript  $i = 1$  to  $K$ , where  $K$  represents the total number of observations. To test the Miller-similarity of the media, the water retention data ( $\theta_i, h_i$ ) were scaled by multiplying measured capillary pressure head values ( $h_i$ ) by media scaling factors,  $f_M$  (Miller and Miller, 1956):

$$h_i^* = f_M h_i \quad [2]$$

where  $h_i^*$  is the scaled capillary pressure head, and the subscript  $M$  represents the four Accusand grades. The media scaling factors were computed using the effective particle diameters

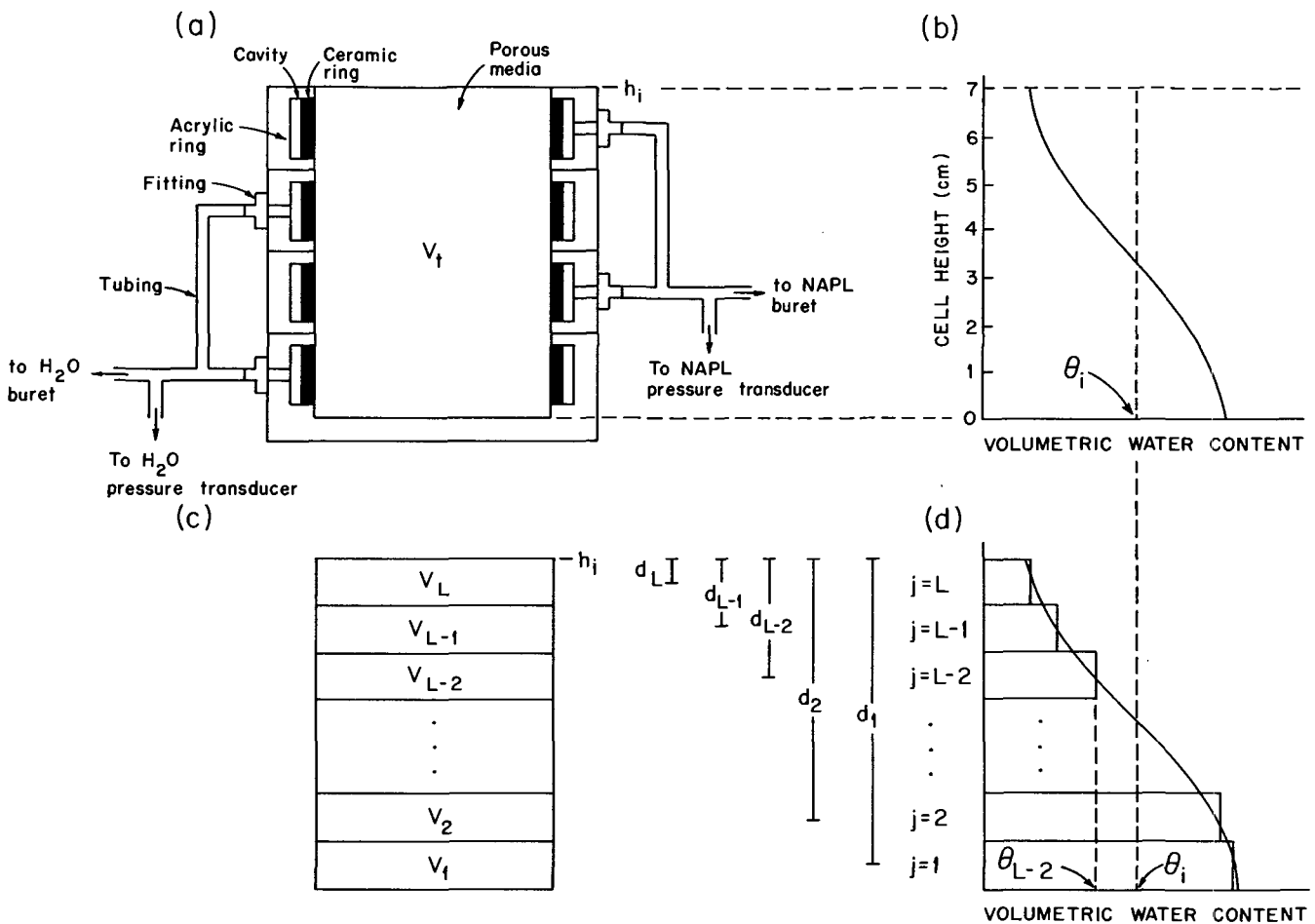


Fig. 1. Experimental apparatus and numerical correction for water retention measurements: (a) retention cell, (b) actual water content distribution, (c) numerical subdivision of retention cell, (d) approximated water content distribution using numerical correction method.

$d_{50}$  for each sand grade. Using the effective particle diameter for the 20/30 sand ( $d_{50,20/30}$ ) as a reference:

$$f_M = d_{50,M}/d_{50,20/30} \quad [3]$$

Effective particle diameters were determined from the particle-size distributions; 50% by weight of the particles have diameters smaller than  $d_{50}$ .

The water retention data were fit to the widely used van Genuchten model (van Genuchten, 1980):

$$\Theta = \left[ \frac{1}{1 + (\alpha h)^n} \right]^m \quad [4]$$

where  $\alpha$  and  $n$  are fitting parameters,  $m = 1 - 1/n$ , the capillary pressure head  $h$  is assumed to be positive, and  $\Theta$  is the effective water saturation, defined as:

$$\Theta = (\theta - \theta_{ir})/(\theta_s - \theta_{ir}) \quad [5]$$

where  $\theta_{ir}$  is the irreducible volumetric water content and  $\theta_s$  is the saturated volumetric water content. Equations [4] and [5] can be combined to obtain a functional relationship between  $\theta$  and  $h$  (van Genuchten, 1980). To fit Eq. [4] to our experimental data ( $V_{w,i}$ ,  $h_i$ ), we combined Eq. [1], [4], and [5] to obtain:

$$\hat{V}_{w,i} = V_t \left\{ \phi - \left[ \frac{1}{1 + (\alpha h_i)^n} \right]^m (\theta_s - \theta_{ir}) - \theta_{ir} \right\} \quad [6]$$

where  $\hat{V}_{w,i}$  is the predicted value of  $V_{w,i}$ . The advantage of writing Eq. [6] in terms of  $V_{w,i}$  rather than  $\theta_i$  will become apparent shortly. The parameters  $\alpha$  and  $n$  were obtained by fitting Eq. [6] to the experimental water retention data ( $V_{w,i}$ ,  $h_i$ ) using a nonlinear least squares routine, minimizing the sum of the squared differences between measured and predicted cumulative volumes of water removed from the cell:

$$\min \left[ \sum_{i=1}^K (V_{w,i} - \hat{V}_{w,i})^2 \right] \quad [7]$$

### Corrections to Water Retention Data

Using Eq. [1] to compute  $\theta_i$  from  $V_{w,i}$  implies the assumption that the volumetric water content is vertically uniform throughout the porous media. However, vertical variation in capillary pressure head within the retention cell creates a non-uniform vertical distribution of volumetric water content (Fig. 1b). While the assumption of vertically uniform distribution of volumetric water content within the cell is reasonable for many soils, for porous media with extremely narrow particle-size distributions, such as the Accusand grades used here, it can create significant errors in the analysis of experimental water retention data. To retroactively compensate for these errors, we developed a numerical technique, based on the van Genuchten (1980) retention model (Eq. [4]), to correct fitted water retention curve parameters to account for non-uniform vertical water content distributions during water retention experiments. A more general computational procedure to correct multiphase fluid capillary pressure-saturation data was recently proposed by Liu and Dane (1995). To obtain corrected retention parameters, they used the Brooks-Corey (1964) function in their computational procedure, with  $\Theta = (h_d/h)^\lambda$  for  $h \geq h_d$ , and  $\Theta = 1$  for  $h < h_d$ , where  $h_d$  is the displacement capillary pressure head and  $\lambda$  is a fitting parameter.

In our approach, the retention cell is imagined to be subdivided

into a set of  $L$  horizontal layers (Fig. 1c). Layer  $j$  has a total volume  $V_j$ , so that

$$\sum_{j=1}^L V_j = V_t \quad [8]$$

The capillary pressure head for any layer can be directly calculated from the measured capillary pressure head  $h_i$  and the vertical distance  $d_j$  between the top surface of the retention cell (the reference point for  $h_i$  in our experiments) and the center of the layer (Fig. 1c). Similar to Eq. [6], the cumulative water volume removed from the cell can be predicted by summing the predicted cumulative water volumes removed from each layer  $\hat{V}_{w,j}$  using:

$$\hat{V}_{w,i} = \sum_{j=1}^L \hat{V}_{w,j} = V_t \sum_{j=1}^L \left( \phi - \left\{ \frac{1}{1 + [\alpha(h_i - d_j)]^n} \right\}^m (\theta_s - \theta_{ir}) - \theta_{ir} \right) \quad [9a]$$

$$\text{for } h_i - d_j > 0 \quad [9a]$$

$$\hat{V}_{w,j} = 0 \quad \text{for } h_i - d_j \leq 0 \quad [9b]$$

Equation [9] was fit to the experimental water retention data using a nonlinear least squares routine to obtain improved estimates for  $\alpha$  and  $n$  by minimizing the sum of the squared differences between measured and predicted cumulative volumes of water removed from the cell (Eq. [7]).

### Air-NAPL-Water Saturation-Pressure Measurements

Three-phase air-NAPL-water S-P characterization was performed using Soltrol as NAPL and distilled water as the aqueous phase employing the method of Lenhard (1992). The S-P measurements were performed in the three-phase retention cell (Fig. 1a) with both water and NAPL rings unclamped. Prior to conducting the experiments, both water and NAPL pressure transducers were calibrated with the respective free liquid surface set to the upper sand surface. All subsequent water and NAPL capillary pressure head measurements were thus made in reference to that location (Fig. 1a). Porous media packing was conducted in the same fashion as for water retention measurements. Three-phase S-P data were obtained from simultaneous measurements of water and NAPL capillary pressure heads as a function of cumulative volumes of water and NAPL drained from or imbibed into the porous media.

At the beginning of each experiment, water was drained from the porous medium by increasing the external vacuum connected to the water rings. Once the porous medium was drained to a water saturation  $S_w \approx 0.10$ , where  $S_w = \theta/\phi$ , a wetting sequence was initiated by lowering the applied vacuum incrementally and allowing water to imbibe into the porous medium. At a water saturation  $S_w \approx 0.55$ , a known volume of NAPL was imbibed through the NAPL rings, thus changing the system from a two-phase air-water to a three-phase air-NAPL-water system. Thereafter, another draining sequence was initiated by allowing water to drain from the porous medium. Finally, water was again allowed to imbibe into the porous medium until the porous medium was apparently liquid saturated, i.e., free NAPL started to become visible at the surface of the retention cell. Fitted three-phase S-P model parameters (Lenhard, 1992) were obtained from measured S-P data using a nonlinear least squares routine.

## Saturated and Unsaturated Hydraulic Conductivity Measurements

One-dimensional column experiments were performed in triplicate to measure saturated and unsaturated hydraulic conductivities for each Accusand grade. The experimental device consisted of a vertical brass column (75 cm high by 5.4 cm i.d.), equipped with eight tensiometers spaced 10 cm apart along the column length. Wire screens (200 mesh) were used to retain the sand at each end of the column. The column was packed by pouring air-dry sand into the upper end of the column through a funnel containing a set of coarse sieves to randomize the particle motion. The funnel and column were electrically grounded during packing to reduce electrostatic charges on the sand particles in order to facilitate a more homogeneous packing. Porosities were computed for each packing from the mass of sand utilized, the particle density, and the total column volume. The column was then flushed with CO<sub>2</sub> gas followed by slow water saturation from the lower end to minimize gas entrapment in the porous medium during the initial water imbibition. Since CO<sub>2</sub> gas has a higher water solubility than air, any initially entrapped CO<sub>2</sub> gas was assumed to dissolve in the aqueous phase, thus creating an initial condition of complete water saturation within the porous medium.

Measurements of saturated hydraulic conductivity were performed during upward flow using the constant-head method (Klute and Dirksen, 1986). The water flow rate into the lower end of the column was controlled with a pump; the upper end of the column was maintained at a constant head by an overflow reservoir. For each packing, measurements of capillary pressure head were performed at three different flow rates. Values of saturated hydraulic conductivity,  $K_{sat}$ , were computed using Darcy's law for all pairs of adjacent tensiometers from measured capillary pressure heads, known tensiometer elevations, and the water flow rates. Average  $K_{sat}$  values were computed for each flow rate, giving a total of nine  $K_{sat}$  values per Accusand grade.

To test the Miller-similarity of the four Accusand grades for  $K_{sat}$ , scaling was performed by dividing average  $K_{sat}$  values by their squared effective particle diameter (Miller and Miller, 1956):

$$K_{sat,M}^* = K_{sat,M}/(d_{50,M})^2 \quad [10]$$

where  $K_{sat}^*$  is the scaled average saturated hydraulic conductivity.

Measurements of unsaturated hydraulic conductivity were conducted immediately following  $K_{sat}$  measurements using the steady-state flux control method (Klute and Dirksen, 1986). After completion of  $K_{sat}$  measurements, the flow through the column was reversed by connecting the pump to the upper end of the column and the constant-head reservoir to the lower end of the column. The column remained fully water saturated during this procedure. To ensure controlled flow conditions at the column bottom, the free water surface of the constant-head reservoir was kept slightly above the outlet port. Downward flow was initiated at a flow rate previously calculated to be sufficient to maintain complete water saturation. The flow rate was then reduced in a series of steps. For each step, measurements of capillary pressure head and water flow rate were conducted when measured capillary pressure heads appeared constant. Using Darcy's law, values of unsaturated hydraulic conductivities,  $K_{unsat}$ , were computed for adjacent tensiometers from measured capillary pressure head values, known tensiometer elevations, and measured water flow rates.

Relative hydraulic conductivities,  $K_{rel}$ , were computed for each Accusand grade using:

$$K_{rel,M}(h) = K_{unsat,M}(h)/K_{sat,M} \quad [11]$$

Computed  $K_{rel}$  values were assigned to the average capillary pressure head values for each pair of adjacent tensiometers.

## RESULTS AND DISCUSSION

### Physical and Chemical Characterization

The four Accusand grades are classified as medium to fine sands (ASTM, 1990). The highly uniform character of the four Accusand grades is exhibited by their narrow particle-size distributions (Fig. 2). To assess the batch-to-batch consistency of the sands, we computed averages and standard deviations of effective particle diameters ( $d_{50}$ ) and uniformity coefficients ( $d_{60}/d_{10}$ , where 60 and 10% by weight of particles have diameters smaller than  $d_{60}$  and  $d_{10}$ , respectively) from sieve analyses conducted by the manufacturer over 3 yr. The small standard deviations for effective particle diameters and uniformity coefficients indicate a high batch-to-batch consistency for all four Accusand grades (Table 1). Particle densities are similar to that of pure quartz. The high sphericity of the Accusand grades increases experimental reproducibility by minimizing porosity variations between consecutive packings. All Accusand grades consisted essentially of quartz with only trace levels of metals (Table 1); low organic matter content and small cation-exchange capacity were additional features common to all four grades of Accusand.

### Water Retention Measurements

As a result of their narrow particle-size distributions, measured water retention curves featured well-defined air entry pressures (Fig. 3). The close agreement of the scaled capillary pressure heads to the unscaled 20/30 Accusand water retention curve demonstrated the Miller-similarity of the Accusand grades. Good agreement was found between measured water retention curves and fitted

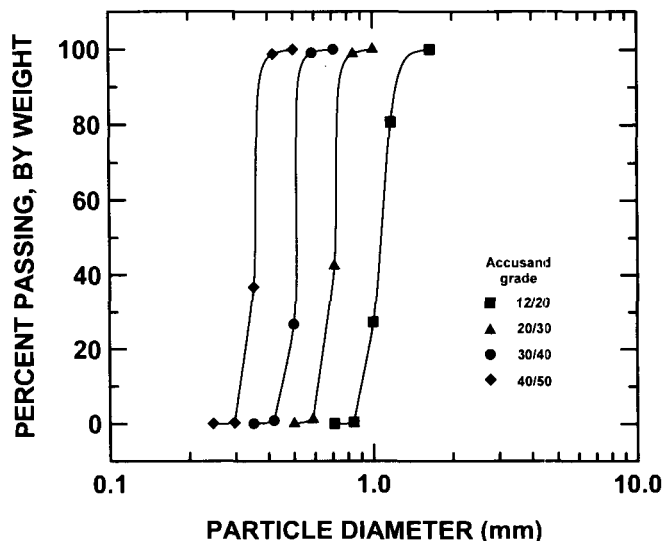


Fig. 2. Particle-size distribution for four Accusand grades.

**Table 1. Physical properties and chemical analyses for four Accusand grades.**

	12/20	20/30	30/40	40/50
<b>Physical properties</b>				
Particle diameter $d_{50}$ (mm)	1.105 ± 0.014†	0.713 ± 0.023	0.532 ± 0.003	0.359 ± 0.010
Uniformity coefficient $d_{60}/d_{10}$	1.231 ± 0.043	1.190 ± 0.028	1.207 ± 0.008	1.200 ± 0.018
Particle sphericity	0.9	0.9	0.9	0.9
Particle density, Mg/m <sup>3</sup>	2.665	2.664	2.665	2.663
<b>Chemical analyses</b>				
Cation-exchange capacity, cmolc/kg	0.60	0.57	0.62	0.67
Total Fe, g/kg	9.31	7.64	7.65	5.58
Fe oxides, g/kg	0.36	0.29	0.34	0.30
Organic C, g/kg	0.3	0.4	0.3	0.3
Total Cd, mg/kg	<7.0	<7.0	<7.0	<7.0
Total Cu, mg/kg	<14.0	<14.0	<14.0	<14.0
Total Pb, mg/kg	<5.0	<5.0	<5.0	<5.0
Total Mn, mg/kg	51.6	43.6	40.3	34.1
Total Zn, mg/kg	9.95	6.98	7.1	6.18

† Averages with standard deviations. Total number of sieve analyses were 19 for 12/20, 170 for 20/30, 9 for 30/40, and 4 for 40/50 sand.

van Genuchten retention functions for all four Accusand grades (Table 2), with coefficients of multiple determination  $R^2 > 0.99$  in all cases.

### Corrections to Water Retention Data

Fitting parameters  $\alpha$  and  $n$  obtained with Eq. [6] and [9] were significantly different (Table 2), i.e., larger values of  $\alpha$  and  $n$  were obtained when our numerical correction technique (Eq. [9]) was employed. The values of  $\alpha$  and  $n$  obtained with Eq. [9], and hence the shape of the fitted water retention curves, depended on the number of layers used to subdivide the retention cell (Fig. 4). Fitted values of  $\alpha$  and  $n$  increased as the number of layers increased. Significant differences in  $\alpha$  and  $n$  existed between the uncorrected ( $L = 1$ ) fit and the correction with three layers. Small differences in  $\alpha$  and  $n$  were observed for  $L = 3$  to 7, and negligible differences in  $\alpha$  and  $n$  existed for  $L = 7$  to 14, resulting in fitted water retention curves that were graphically indiscernible (Fig. 4). Since the correction method could be easily

implemented on a standard computer spreadsheet, a higher resolution was chosen for the data presented in this study (14 layers), equivalent to 0.5-cm-thick layers (Table 2).

Large differences between uncorrected and corrected fitting parameters illustrated the importance of the correction for modeling water retention curves for these sands. When employing Eq. [4] and [5] to predict  $\theta$  from  $h$ , errors in volumetric water content as high as 70% could result from using uncorrected fitting parameters (Fig. 4). However, the magnitude of these errors will depend on the height of the retention cell, i.e., they decrease with decreasing cell height, and the porous medium pore-size distribution. Smaller errors can be expected in less uniform porous media. Note that these errors are not restricted to the retention cell used in our experiments, but also apply to water retention experiments conducted using standard Tempe cells (Klute, 1986). The basic approach for the numerical correction employed in this study can be modified for use with alternate retention functions, e.g., the Brooks-Corey function (Brooks and Corey, 1964). Corrected Brooks-Corey fitting parameters for the four Accusand grades are provided in Table 2.

### Air-NAPL-Water Saturation-Pressure Measurements

Three-phase S-P model parameters (Lenhard, 1992; Parker and Lenhard, 1987) for water and Soltrol were

**Table 2. Uncorrected and corrected van Genuchten and corrected Brooks-Corey fitting parameters of water retention data (main drainage curves) for four Accusand grades.**

Accusand grade	van Genuchten		van Genuchten		Brooks-Corey corrected†			
			uncorrected	corrected†	corrected†	corrected†	$h_0$	$\lambda$
	$\theta_s$	$\theta_{ir}$	$\alpha$	$n$	$\alpha$	$n$	cm	
	— m <sup>3</sup> /m <sup>3</sup> —		cm <sup>-1</sup>		cm <sup>-1</sup>		cm	
12/20	0.348	0.012	0.100	6.54	0.151	7.35	5.42	3.94
20/30	0.348	0.016	0.0744	8.47	0.0995	10.57	8.66	5.57
30/40	0.348	0.018	0.0552	10.54	0.0679	13.10	13.03	6.91
40/50	0.348	0.020	0.0392	11.58	0.0453	12.18	19.37	6.17

† Corrected for nonuniform water content distribution using 14-layer subdivision.

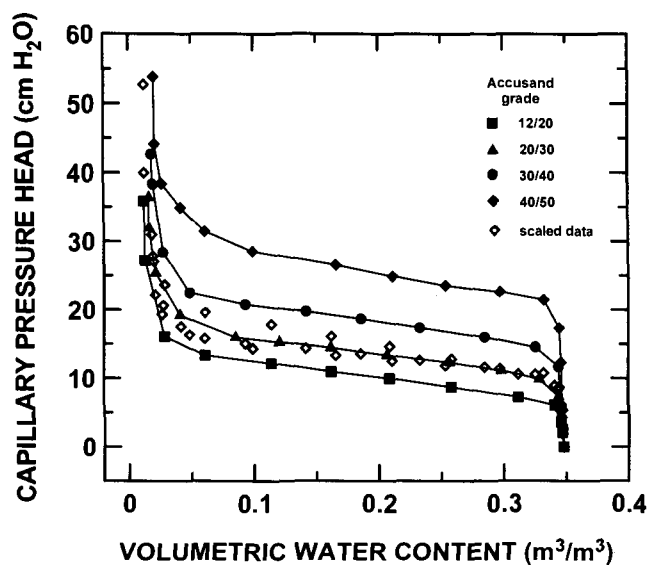


**Fig. 3. Water retention data (main drainage curves) for four Accusand grades. Solid symbols show actual data, solid lines connect consecutive data points, and open symbols represent scaled data.**

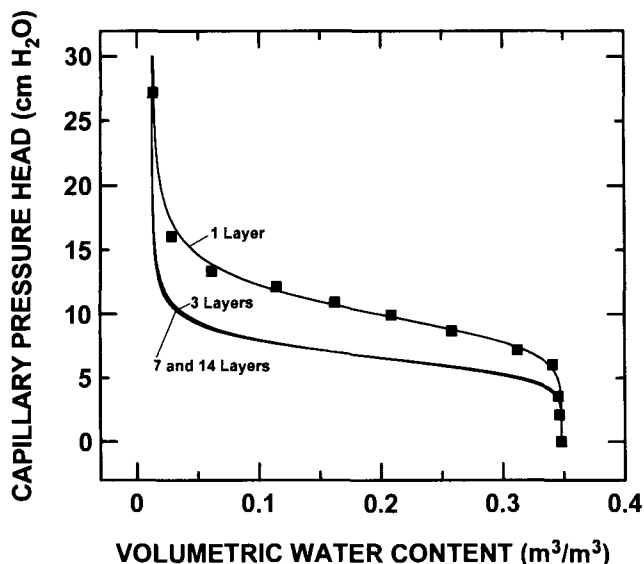


Fig. 4. Effect of numerical correction procedure on fitted Accusand 12/20 water retention function. Solid symbols show measured data and solid lines show fitted van Genuchten (1980) retention functions for subdivision into different numbers of layers.

obtained using the three-phase S-P data. An example of S-P data for Accusand 30/40 is shown in Fig. 5. Water saturation  $S_w$ , and total liquid saturation  $S_t$ , with  $S_t = S_w + S_o$ , where  $S_o$  is the NAPL saturation ( $o$  stands for "oil" and is commonly used in lieu of NAPL), were plotted against scaled capillary pressure heads, measured on a water-height-equivalent basis. Scaling of capillary pressure heads was conducted by multiplying air-NAPL capillary pressure heads with the air-NAPL scaling factor,  $\beta_{ao}$ , and NAPL-water capillary pressure heads with the NAPL-water scaling factor,  $\beta_{ow}$  (Table 3). It is due to this scaling of capillary pressure heads that three-phase S-P data appear as a smooth continuation of two-phase S-P data. Other fitted model parameters obtained included van Genuchten (1980) retention parameters  $\alpha_d$ ,  $\alpha_i$ , and  $n$ , where  $\alpha_d$  and  $\alpha_i$  were modified parameters associated with the main drainage and main imbibition branches, respectively. Following investigations of Kool and Parker (1987),  $n$  was assumed constant for drainage and imbibition branches. In addition, the maximum residual air saturation associated with the main air-water imbibition branch,  $S_{ar}(aw)$ , the maximum residual air saturation associated with the main air-NAPL imbibition branch,  $S_{ar}(ao)$ , and the maximum residual NAPL saturation associated with the main NAPL-water imbibition branch,  $S_{or}(ow)$ , were obtained using the inverse of an algorithm proposed by Land (1968) to determine entrapped nonwetting fluid saturations. Increasing fluid wettability in the order air < NAPL < water was assumed for our experiments. Good agreement between experimental data and the fitted model was observed for all four Accusand grades, indicated by high  $R^2$  (Table 3).

Similar to water retention data, three-phase S-P data were analyzed assuming vertically uniform fluid saturation distributions. No numerical correction during fitting was attempted to correct three-phase model parameters for conditions of vertical non-uniform fluid saturation

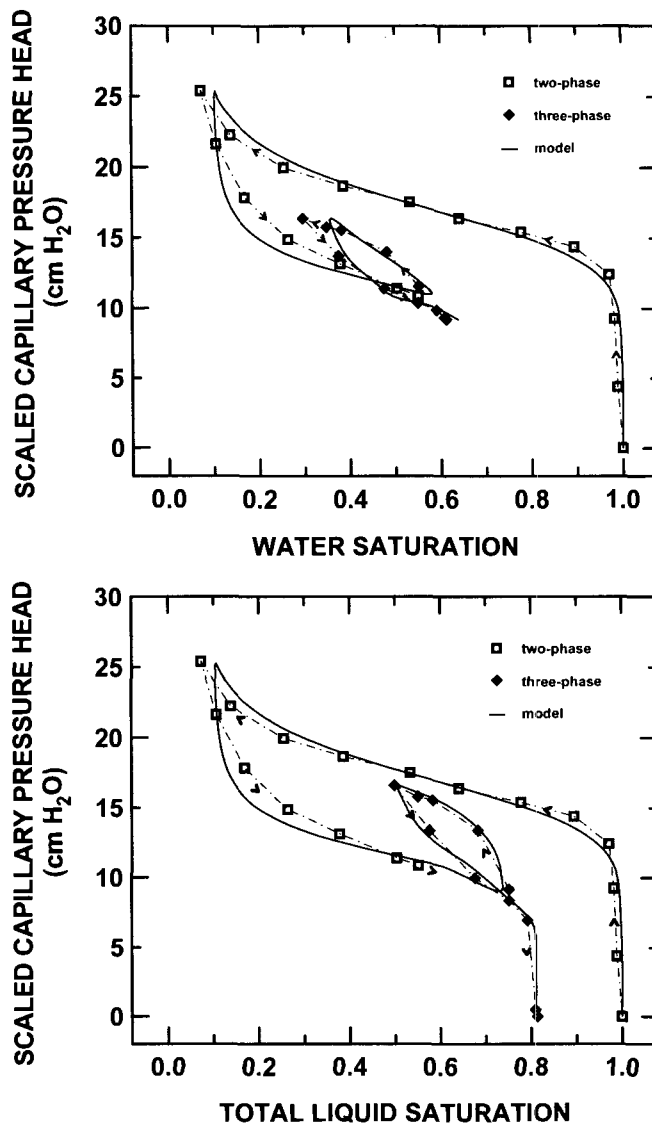


Fig. 5. Three-phase air-non-aqueous-phase liquid (NAPL)-water saturation-pressure (S-P) data for Accusand 30/40 using Soltrol 220: (a) water S-P data, (b) total liquid S-P data. Open squares represent saturations in two-phase air-water system, solid diamonds represent saturations in three-phase air-NAPL-water system, arrows indicate saturation path, and solid lines show model (Lenhard, 1992) prediction.

distributions and no rigorous analysis of parameter sensitivity to errors in interpreting S-P data in this manner is given here. By similarity to water retention measurements, it is reasonable to assume that water retention parameters ( $\alpha_d$ ,  $\alpha_i$ ,  $n$ ) are significantly affected by these errors (Table 3). Scaling factors ( $\beta_{ao}$ ,  $\beta_{ow}$ ) may be more robust because measurements of NAPL and water capillary pressure heads were made relative to the same reference point ( $h_i$ , Fig. 1). Residual nonwetting fluid saturations [ $S_{ar}(aw)$ ,  $S_{ar}(ao)$ ,  $S_{or}(ow)$ ] were determined from fluid drainage and imbibition sequences (Lenhard, 1992). Identical scaled capillary pressure heads existed at start and end points of these sequences, rendering these parameters more robust to errors due to non-uniform vertical saturation distributions.

Corrected water retention parameters  $\alpha$  and  $n$  obtained

**Table 3. Three-phase air–non-aqueous-phase liquid (NAPL)–water model parameters for four Accusand grades obtained from saturation–pressure data using distilled water and Soltrol 220 as the NAPL.**

Accusand grade	$\theta$		uncorrected†			corrected‡			$\beta_{ao}$	$\beta_{ow}$	$S_{ur}(aw)$	$S_{ur}(ao)$	$S_{or}(ow)$	$R^2§$
	$\theta_s$	$\theta_r$	$\alpha_d$	$\alpha_i$	$n$	$\alpha_d$	$\alpha_i$	$n$						
	— $m^3/m^3$ —		— $cm^{-1}$ —			— $cm^{-1}$ —								
12/20	0.348	0.012	0.105	0.144	6.75	0.151	0.217	7.35	2.38	1.76	0.08	0.17	0.16	0.98
20/30	0.348	0.016	0.0787	0.117	8.07	0.0995	0.156	10.57	2.21	1.60	0.11	0.11	0.15	0.98
30/40	0.348	0.018	0.0584	0.0880	8.35	0.0679	0.108	13.10	2.20	1.82	0.11	0.16	0.17	0.99
40/50	0.348	0.020	0.0421	0.0714	9.34	0.0453	0.0825	12.18	2.17	1.62	0.10	0.10	0.12	0.93

† Not corrected for nonuniform fluid saturation distribution.

‡ Corrected parameters recommended for modeling purposes.

§ Coefficient of multiple determination for uncorrected fit.

for two-phase air–water systems (Table 2) were directly employed as corrections for parameters  $\alpha_d$  and  $n$  in Table 3. To obtain corrected values of  $\alpha_i$  for each Accusand grade (Table 3), we multiplied the uncorrected values of  $\alpha_i$  by the ratio of  $\alpha_{corrected}/\alpha_{uncorrected}$  (Table 2). Based on our findings for fitted water retention curves (Fig. 4), we recommend the use of corrected water retention parameters for three-phase fluid flow modeling purposes (Table 3).

### Saturated and Unsaturated Hydraulic Conductivity Measurements

Measured  $K_{sat}$  exhibited good reproducibility, indicated by small standard deviations (Table 4). However, consistent packing of the experimental device (to similar porous media porosities) was required to obtain such reproducibility. Porosities in our experiments ranged from 0.33 to 0.35. Measured  $K_{sat}$  values for the four Accusand grades (Table 4) agreed well with typical  $K_{sat}$  values for uniform sands (Bear, 1972). In preliminary experiments, we obtained porosities of approximately 0.40 (funnel and column were not electrically grounded during packing) and  $K_{sat}$  values measured were larger by nearly a factor of two than the values reported in Table 4. This illustrates the critical importance of achieving similar porosities in experimental devices when employing the data presented in this study.

Scaling of average  $K_{sat}$  values also illustrated the Miller-similarity of the four Accusand grades (Table 4). Although a slight trend existed in the scaled data ( $K_{sat}^*$ ) for the four Accusand grades, an average  $K_{sat}^*$  value for the four Accusand grades of 29.9 cm/min was computed with a standard deviation of only 3.80 cm/min.

Abrupt changes in  $K_{rel}$ , computed from  $K_{unsat}$  and  $K_{sat}$  measurements (Eq. [11]), were observed within a narrow

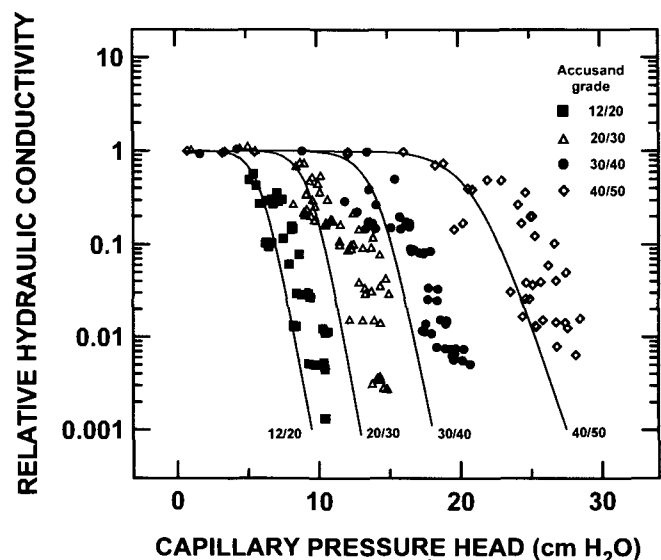
**Table 4. Average saturated hydraulic conductivities ( $K_{sat}$ ) and scaled saturated hydraulic conductivities ( $K_{sat}^*$ ) for four Accusand grades.**

Accusand grade	$K_{sat}$		$K_{sat}^*$
	$x$	SD	
	— $cm/min$ —		
12/20	30.19	1.00	24.73
20/30	15.02	0.31	29.55
30/40	8.94	0.31	31.59
40/50	4.33	0.11	33.60

range of applied capillary pressure heads (Fig. 6). We tested the agreement between computed  $K_{rel}$  data and values predicted by the van Genuchten–Mualem model (van Genuchten, 1980):

$$K_{rel}(h) = \frac{\left\{1 - (\alpha h)^{n-1} [1 + (\alpha h)^n]^{-m}\right\}^2}{[1 + (\alpha h)^n]^{m/2}} \quad [12]$$

with  $m = 1 - 1/n$ , using corrected water retention parameters  $\alpha$  and  $n$  (Table 2) as input parameters in Eq. [12]. The shapes of the predicted relative conductivity functions reproduced those obtained experimentally (Fig. 6). However, a shift of 1.5 to 2.5 cm in capillary pressure head existed on average between model predictions and computed  $K_{rel}$  data. This led to discrepancies between computed and predicted  $K_{rel}$  values up to approximately one order of magnitude (Fig. 6). The observed shift in capillary pressure head may be due to experimental error in obtaining averaged capillary pressure head data, the assumption that capillary pressure head varied linearly between tensiometers, and the high sensitivity of  $K_{rel}$  to small changes in capillary pressure head. In addition, porosities in hydraulic conductivity experiments were

**Fig. 6. Relative hydraulic conductivities ( $K_{rel}$ ) for four Accusand grades. Symbols represent measured data, solid lines represent predicted values of  $K_{rel}$  using the van Genuchten–Mualem model (Eq. [12]) and corrected water retention parameters  $\alpha$  and  $n$  (Table 2).**

slightly smaller on average (0.33–0.35) than in water retention experiments. Thus, parameters  $\alpha$  and  $n$  determined from water retention experiments may not have exactly reflected experimental conditions during hydraulic conductivity measurements, i.e., water retention of the porous media was slightly underpredicted during hydraulic conductivity measurements, and may be responsible for underpredicting experimentally determined  $K_{rel}$  data for any given capillary pressure head (Fig. 6). Nonetheless, the van Genuchten–Mualem model (van Genuchten, 1980) appears adequate for predicting the unsaturated hydraulic conductivities of the media for numerical modeling applications, provided that modeled packing densities match those of our water retention experiments.

When uncorrected water retention parameters (Table 2) were used in Eq. [12] to predict  $K_{rel}$  (data not shown), poor agreement between computed and predicted values of  $K_{rel}$  was observed. The predictive models of van Genuchten–Burdine (van Genuchten, 1980), Brooks–Corey–Burdine (Brooks and Corey, 1964), and Gardner (Gardner, 1958) did not exhibit improved agreement with the computed  $K_{rel}$  data (data not shown).

## CONCLUSIONS

We presented a comprehensive set of hydrologically relevant parameters for four commercially available silica sands. The sands featured narrow particle-size distributions and were found very amenable to Miller scaling for both hydrostatic (water retention) and hydrodynamic (saturated hydraulic conductivity) parameters.

Parameterization of water retention data for four Accusand grades was obtained by fitting a general equation (van Genuchten, 1980) to the experimental data. A numerical correction procedure was outlined to be used during the fitting of the general equation to compensate for an interpretation error in the experimental water retention data due to a commonly made assumption. The error resulted from nonuniform vertical distributions of volumetric water content due to hydrostatic pressure differences in the experimental device. This numerical correction procedure is not restricted to the water retention function used in this study, but may be applied to a variety of functional forms.

Three-phase S–P model parameters (Lenhard, 1992) were obtained for a widely used model NAPL. Similar to water retention data, three-phase S–P data were analyzed, implying the assumption of vertically uniform fluid saturation distributions. Numerical correction of three-phase model parameters for errors in interpretation of S–P data was limited to water retention parameters, and was conducted by employing previously corrected two-phase water retention data. To rigorously assess the influence of these errors on all three-phase model parameters, a more specific analysis is required.

Reasonable agreement was found between measured and predicted values of relative hydraulic conductivity using corrected water retention fitting parameters in the van Genuchten–Mualem model (van Genuchten, 1980). Poor agreement for uncorrected parameters indicated the

importance of the numerical correction procedure for the porous media used in this study.

The four Accusand grades appear to be a suitable set of media for a broad range of flow and transport studies due to their well-defined hydrologic properties, high batch-to-batch consistency, availability in large quantities, and chemical purity, as well as their Miller-similarity.

## ACKNOWLEDGMENTS

This work was funded by the U.S. Department of Energy (DOE) under contract no. DE-FG06-92-ER61523 under the Subsurface Science Program. We would like to thank Dr. Robert J. Lenhard, Sultan Qaboos University, Sultanate of Oman, for valuable technical and material assistance. We would also like to thank Dr. Raina M. Miller, University of Arizona, for conducting the chemical analyses on the media. Thanks also to Jenny Curtis, U.S. Geological Survey, who performed the He pycnometer measurements of particle density and to Darren Lerner for helping conduct the conductivity measurements.

## REFERENCES

- American Petroleum Institute. 1986. Recommended practices for testing sand used in gravel packing operations. API RP-58. Am. Pet. Inst., Washington, DC.
- Artiola, J.F. 1990. Determination of carbon, nitrogen, and sulfur in soils, sediments, and wastes: a comparative study. *Int. J. Environ. Anal. Chem.* 41:159–171.
- ASTM. 1987. Standard specification for wire-cloth sieves for testing purposes. ASTM E11-87, p. 13–16. *In* 1993 Annual book of ASTM standards. Vol. 14.02. ASTM, Philadelphia, PA.
- ASTM. 1990. Standard test method for particle-size analysis of soils. ASTM D 422-63, p. 93–99. *In* 1993 Annual book of ASTM standards. Vol. 04.08. ASTM, Philadelphia, PA.
- Ayral, A., J. Phalippou, and T. Woignier. 1992. Skeletal density of silica aerogels determined by helium pycnometry. *J. Mater. Sci.* 27:1166–1170.
- Bear, J. 1972. *Dynamics of fluids in porous media*. Dover, New York.
- Brooks, R.H., and A.T. Corey. 1964. Hydraulic properties of porous media. *Hydrol. Pap.* 3. Colorado State Univ., Fort Collins.
- Cary, J.W., C.S. Simmons, and J.F. McBride. 1994. Infiltration and redistribution of organic liquids in layered porous media. *Soil Sci. Soc. Am. J.* 58:704–711.
- Gardner, W.R. 1958. Some steady-state solutions of the unsaturated moisture flow equation with application to evaporation from a water table. *Soil Sci.* 85:244–249.
- Klute, A. 1986. Water retention: Laboratory methods. p. 635–662. *In* A. Klute (ed.) *Methods of soil analysis*. Part 1. 2nd ed. Agron. Monogr. 9. ASA and SSSA, Madison, WI.
- Klute, A., and C. Dirksen. 1986. Hydraulic conductivity and diffusivity: laboratory methods. p. 687–734. *In* A. Klute (ed.) *Methods of soil analysis*. Part 1. 2nd ed. Agron. Monogr. 9. ASA and SSSA, Madison, WI.
- Kool, J.B., and J.C. Parker. 1987. Development and evaluation of closed-form expressions for hysteretic soil hydraulic properties. *Water Resour. Res.* 23:105–114.
- Land, C. 1968. Calculation of imbibition relative permeability for two- and three-phase flow from rock properties. *Trans. Am. Inst. Min. Metall. Pet. Eng.* 207:149–156.
- Lenhard, R.J. 1992. Measurement and modeling of three-phase saturation–pressure hysteresis. *J. Contam. Hydrol.* 9:243–269.
- Lenhard, R.J., and J.C. Parker. 1988. Experimental validation of the theory of extending two-phase saturation–pressure relations to three-fluid phase systems for monotonic drainage paths. *Water Resour. Res.* 24:373–380.
- Liu, H.H., and J.H. Dane. 1995. Improved computational procedure



- for retention relations of immiscible fluids using pressure cells. *Soil Sci. Soc. Am. J.* 59:1520-1524.
- Miller, E.E., and R.D. Miller. 1956. Physical theory for capillary flow phenomena. *J. Appl. Phys.* 27:324-332.
- Page, A.L., R.H. Miller, and D.R. Keeney. 1982. Methods of soil analysis. Part 2. 2nd ed. *Agron. Monogr.* 9. ASA and SSSA, Madison, WI.
- Parker, J.C., and R.J. Lenhard. 1987. A model for hysteretic constitutive relations governing multiphase flow, 1. Saturation-pressure relations. *Water Resour. Res.* 23:2187-2196.
- U.S. Environmental Protection Agency. 1986. Method EPA 6010. *In* Methods of analysis of hazardous solid wastes. SW-846. 3rd ed. USEPA, Office of Solid Waste., Washington, DC.
- van Genuchten, M.Th. 1980. A closed-form equation for predicting the hydraulic conductivity of unsaturated soils. *Soil Sci. Soc. Am. J.* 44:892-898.